

## Assembly of Shape-Controlled Nanocrystals by Depletion Attraction †‡

Marco Zanella<sup>a</sup>, Giovanni Bertoni<sup>a</sup>, Isabella R. Franchini<sup>a</sup>, Rosaria Brescia<sup>a</sup>, Dmitry Baranov<sup>a</sup>, &  
and Liberato Manna<sup>a</sup> \*

### Supporting information

#### Details on the assembly procedure

Vertical assemblies of rods in this work were obtained using a procedure similar to the one we have recently published [1]. In a typical experiment 50 µl of a toluene solution of nanorods ( $3.3 \times 10^{-5}$  M concentration in nanorods) were placed into a 3 ml glass vial with stirring bar and 1 ml of anhydrous toluene was added to it. Then the additives (Oleic acid or oleylamine) were injected dropwise to the nanorods solution. During additive injection, the resulting solution turned cloudy, and the cloudiness increased over time due to the formation of the assemblies. In the case of oleic acid for example the appearance of cloudiness was observed after additions of about 200 µL of pure oleic acid. At this point the solution was gently centrifuged (2000 rpm) or left decanting overnight. The precipitated assemblies were separated from the supernatant and redispersed in a polar solvent (i.e. ethanol, methanol or isopropanol). TEM grids were prepared by dipping the grids in the dispersion containing the assemblies.

TEM images of the  $\text{Fe}_2\text{P}$ , CdSe and CdSe/CdS rods used for the depletion attraction experiments

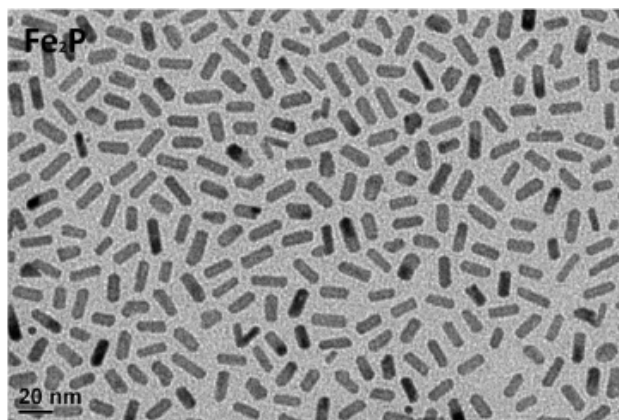


**Fig. S1.** TEM image of the  $\text{Fe}_2\text{P}$  nanorods used for the nanorod assemblies in the work.

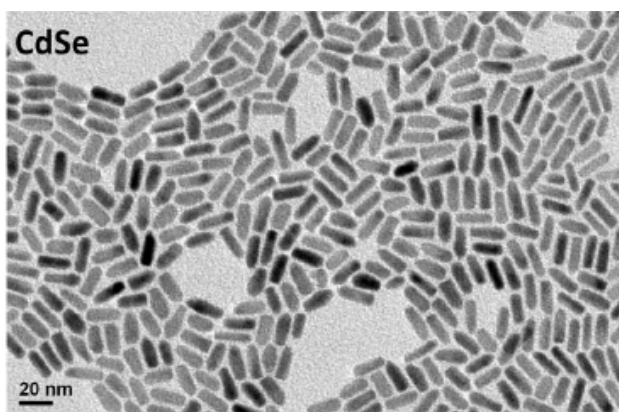


**Fig. S2.** TEM image of the CdSe nanorods used for the nanorod assemblies in the work.

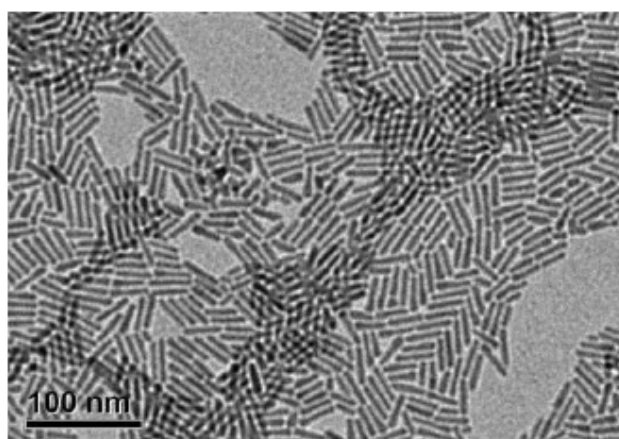


**Fig. S3.** TEM image of the CdSe(spherical core)/CdS (rod-shaped shell) nanorods used for the nanorod assemblies (and cations exchange reactions) in the work.

### X-ray Energy Dispersion Spectrometry (XEDS) analysis of CdSe/CdS rods before and after Cu<sup>+</sup> cation exchange

XEDS line analysis were performed in HAADF-STEM mode (1 nm electron beam) in order to identify the Se-containing core inside CdSe/CdS rods, before and after the cation exchange reaction with Cu<sup>+</sup>. Copper cation exchange on CdSe/CdS rods was performed according to [5]. The analysis performed over different rods highlighted the presence of a small core close to one end of such rods. For correct visualization of the Cu signal after cation exchange, a Ni grid was used to avoid background signal from the standard Cu grids. Two representative XEDS profiles are presented in Fig.S4 and Fig.S5.

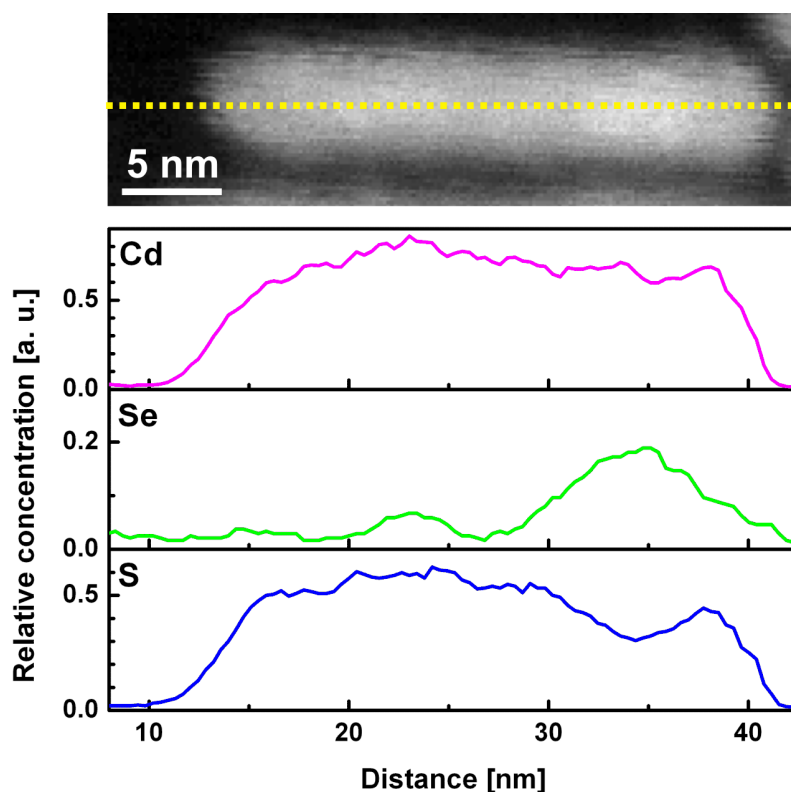


**Fig. S4** XEDS elemental profiles from a CdSe/CdS rod, confirming the presence of a Se-containing core starting ~2 nm from one end of a ~26 nm long rod, and extended for ~6 nm. There is a decrease in the S signal corresponding to the increase in the Se signal due to the presence of the core. The Cd signal is roughly constant along the rod.

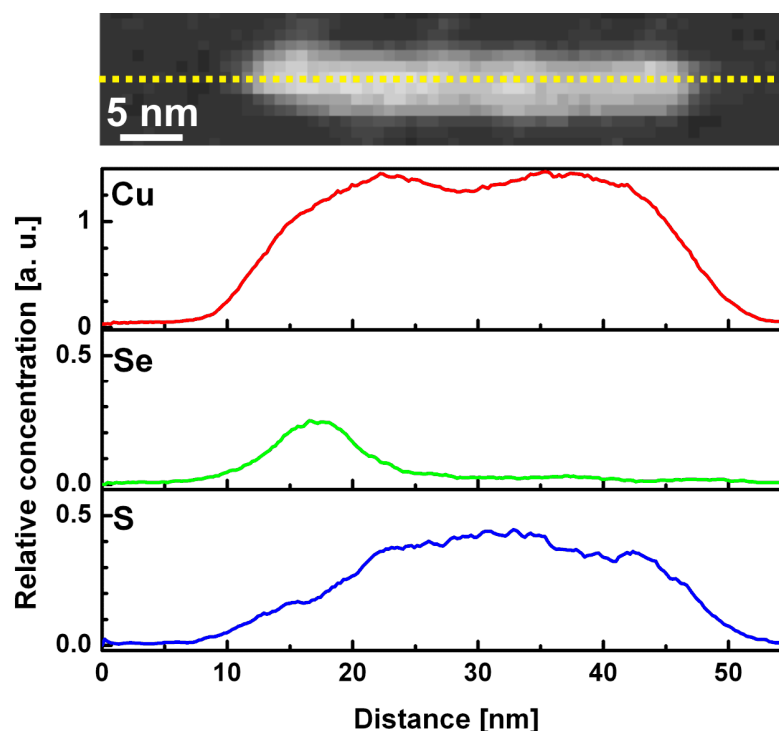


**Fig.S5.** XEDS elemental profiles from a rod as in Fig.S5 but after Cu exchange. The elemental profiles indicate the presence of a Se-containing core starting  $\sim 2$  nm from one end of a  $\sim 34$  nm long rod, extended for  $\sim 7$  nm. There is a weak decrease in the S signal corresponding to the core. The Cu signal is roughly constant along the rod, and not far from the expected  $\text{Cu}_2\text{Se}/\text{Cu}_2\text{S}$  stoichiometry.

### Energy Filtered Transmission Electron Microscopy (EFTEM) analysis of the binary assemblies of vertically aligned nanorods

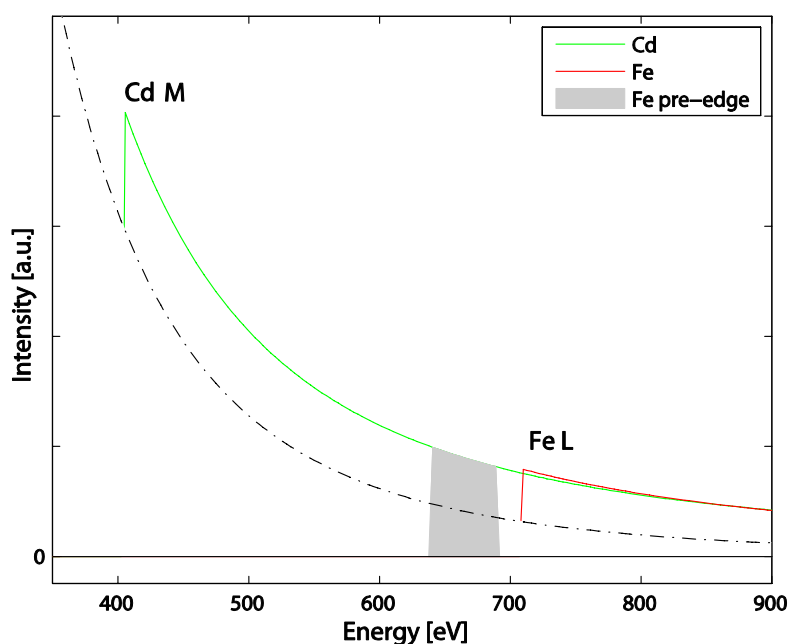
To correctly identify and chemically map each nanorod in both the mixtures of non-assembled nanorods and in the assemblies, energy filtered transmission electron microscopy images (EFTEM) were acquired on a JEOL JEM-2200FS, equipped with a FEG gun and with an Omega filter. Due to the high reactivity of the organic contaminants/surfactants present in the samples under the beam (they burned rapidly when converging the beam, forming a halo of carbon contamination on the illuminated area), the sample was observed at low temperature (liquid nitrogen) using a cryo-holder (Gatan 626.DH), to dissipate the beam energy. Also, a small illumination aperture was used to reduce intensity.

For the assemblies of CdSe and  $\text{Fe}_2\text{P}$  nanorods, the experimental settings above were sufficient for having no contamination on the sample during the 2 minutes needed for acquiring the three images from the Fe L edge at 708 eV (one post edge image and two pre-edge images) in order to compute the Fe elemental map (for simplicity we refer to the  $\text{L}_{2,3}$  edge as L). A 40 eV energy window was used in the experiment.

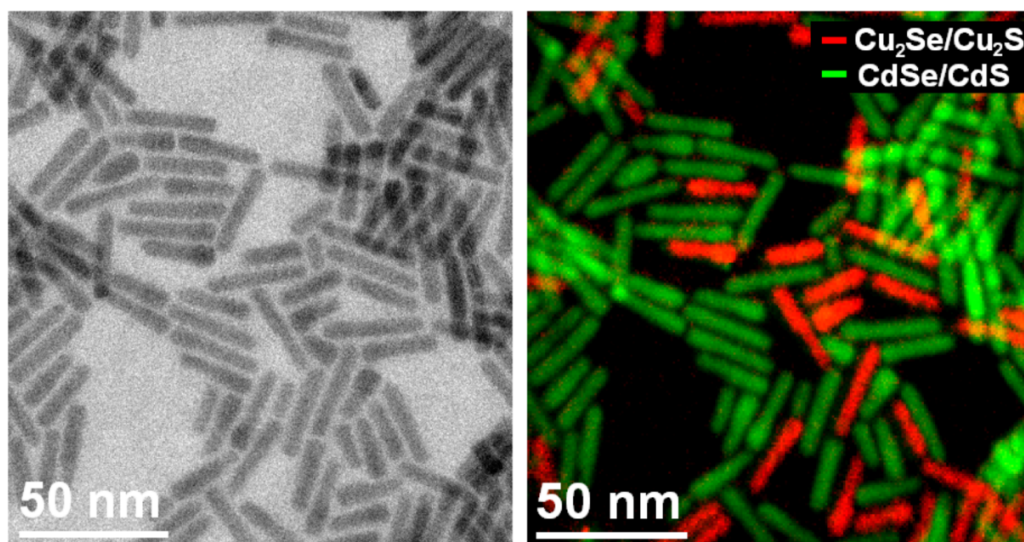


Fig. S6 illustrates how the Fe L pre-edge image mimics the chemical contrast of Cd from CdSe particles, making not necessary the acquisition of a Cd or Se map. A similar behavior is found in the Cu pre-edge image for the mixtures of CdSe/CdS and Cu<sub>2</sub>Se/Cu<sub>2</sub>S nanorods (but with a lower contrast).

For the assemblies of CdSe/CdS and Cu<sub>2</sub>Se/Cu<sub>2</sub>S nanorods, it was not possible to avoid the slow formation of a contaminant halo on the observed areas during the long acquisition times needed for elemental mapping (up to almost 4 minutes in total for each region). In this case, due to the higher complexity of the system, chemical maps of both Cd and Cu were acquired to improve the contrast. EFTEM images were acquired at the Cd M<sub>4,5</sub> edge (M for simplicity) at 404 eV (30 eV energy slit) and at the Cu L edge at 931 eV (40 eV energy slit).



**Fig. S6.** Sketch of the inelastic signal in an EELS experiment on a binary system as Fe<sub>2</sub>P/CdSe. The filtered pre-edge image (grey region in the figure) from the higher energy edge (Fe L in this case) mimics the contrast of the elemental map of Cd (M edge at lower energy), i.e. bright regions correspond to CdSe particles. Computing the Cd map from three images from the Cd M edge is not needed, and the contrast is only partly reduced by the background (dash-dot line). However, a Fe post-edge is not sufficient to uniquely address the Fe<sub>2</sub>P particles. Three images (one post edge and two pre-edge) are needed in this case to compute the contrast corresponding to Fe. Note that a map from the Cd M edge can be noisy due to the high background at lower energy (the carbon signal from the surfactant heavily contributes to it), while the Fe L edge is a good candidate for elemental mapping due to the high signal to background ratio at its energy. A similar contrast should be found also for Cu in the mixture of CdSe/CdS + Cu<sub>2</sub>Se/Cu<sub>2</sub>S rods, but lowered by the concomitant presence of Se and S in both types of nanoparticles (contributing to the background).



**Fig. S7.** Elasticity filtered TEM image (left) and color map after superposition of Cd (from the Cd M edge) and Cu (from the Cu L edge) maps (right) from a mixed sample of CdSe/CdS and  $\text{Cu}_2\text{Se/Cu}_2\text{S}$  nanorods, before superlattice formation. The two species look identical in the TEM image, while they can be easily distinguished in the filtered maps.

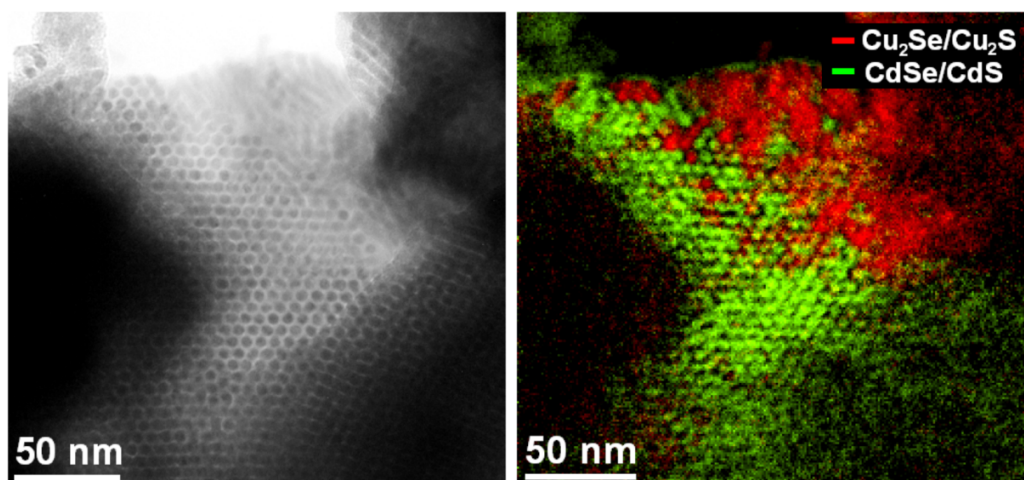


**Fig. S8.** Elasticity filtered TEM image (left) and color map after superposition of Cd and Cu maps (right) from a region of the binary superlattice of CdSe/CdS and  $\text{Cu}_2\text{Se/Cu}_2\text{S}$  nanorods. In this region the clustering of the two types of rods is particularly evident.

#### Shape Selective Separation of various nanorod samples

Shape selective separation was performed by adding an excess of additive (oleic acid, oleylamine or PMMA) to a toluene solution of mixed nanoparticles (i.e. rods-spheres). Also in this case, during additive injection, the resulting solution turned cloudy, and the cloudiness increased over time due to the formation of the assemblies

[1]. The precipitate was then separated from the supernatant by centrifugation, and was then dispersed in fresh solvent and TEM images of it were taken (see figure S9 and S10).

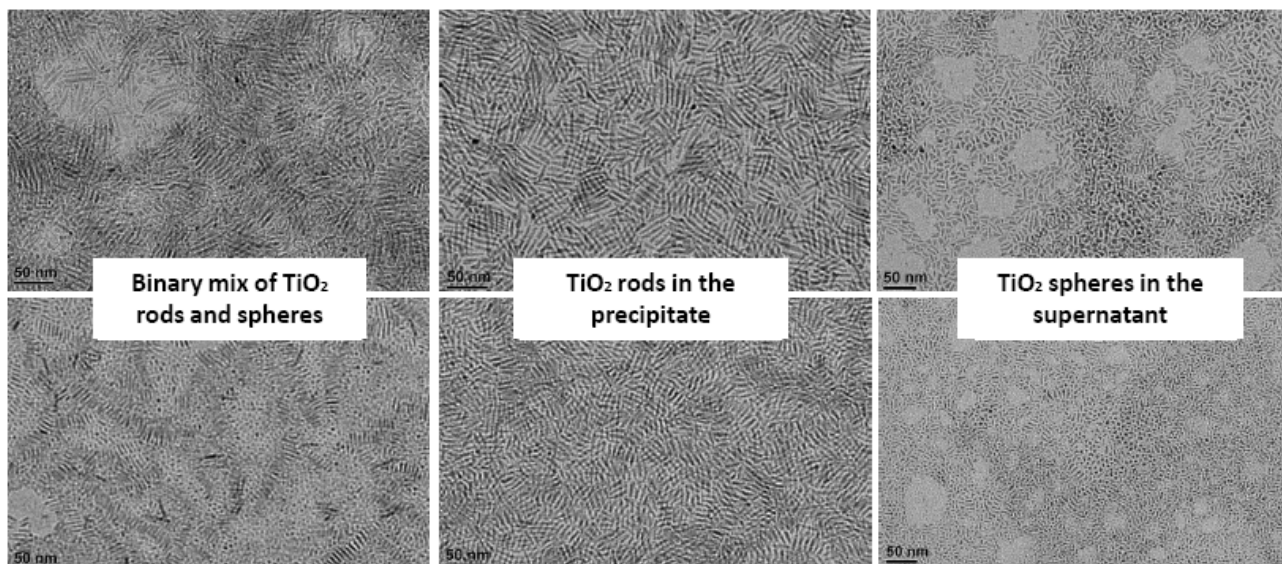


**Fig. S9.** TEM images documenting two different examples of shape selective separation of brookite  $\text{TiO}_2$  rods from  $\text{TiO}_2$  spheres and smaller aspect ratio rods. Smaller rods and spheres were present as byproduct of the rods synthesis. The particles were synthesized according to [2]. In figure a,b and c the average length of the rods was  $28.8 \pm 5.6 \text{ nm}$ , and the average diameter of the spheres was  $3.0 \pm 0.8 \text{ nm}$ . In figure d, e and f the rod length was  $21.9 \pm 3.4 \text{ nm}$  with spheres having average diameter equal to  $3.3 \pm 0.6 \text{ nm}$ .

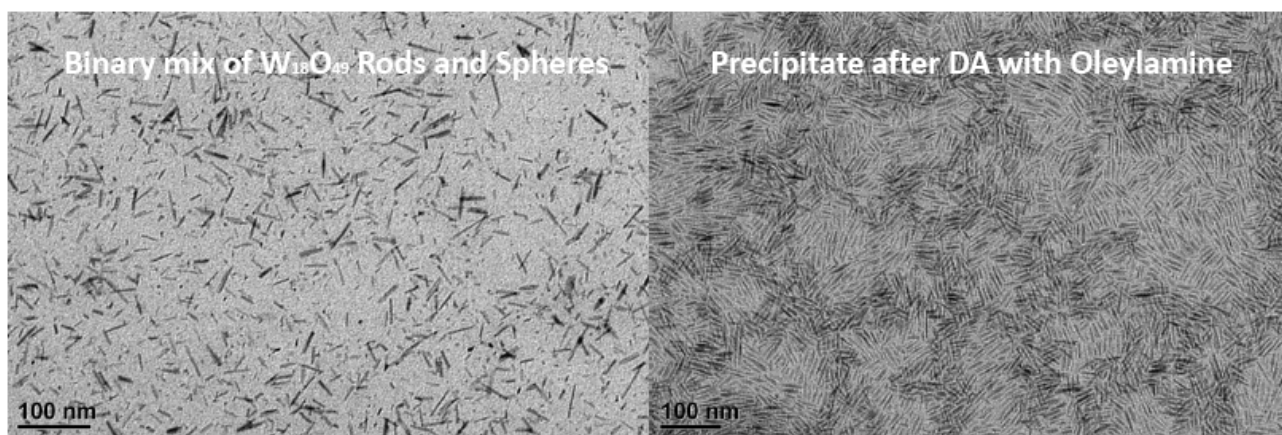


**Fig. S10.** TEM images documenting the shape selective separation of  $\text{W}_{18}\text{O}_{49}$  rods from tungsten oxide spheres using oleylamine as additive. Spheres were present as byproduct of the rod synthesis. Rods were synthesized according to [3].

### Formation of tetrapods and octapods 3D assemblies via depletion attraction

Tetrapods and octapods 3D assemblies can be found in solution when an excess of additive (oleic acid, oleylamine or PMMA) is added to the nanoparticles dissolved in toluene. These clusters can be separated from particles left in solution by centrifugation or decantation. After the separation tetrapods (Figure S11) and octapods (Figure S12) assemblies are stable in polar organic solvents such as ethanol, methanol and isopropanol.

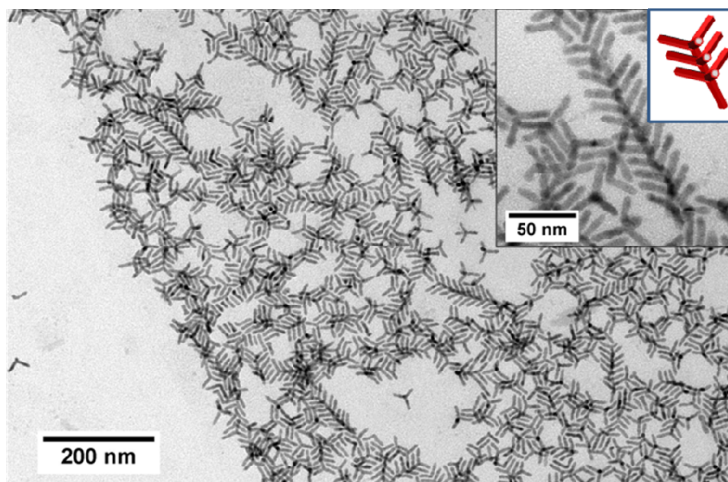


**Fig. S11.** *ZnTe@CdTe tetrapods drop-casted onto a TEM grid from ca. 0.14M PEG-MA (average  $M_n = 526$ , density of PEG-MA is 1.101 g/ml) solution in toluene.*

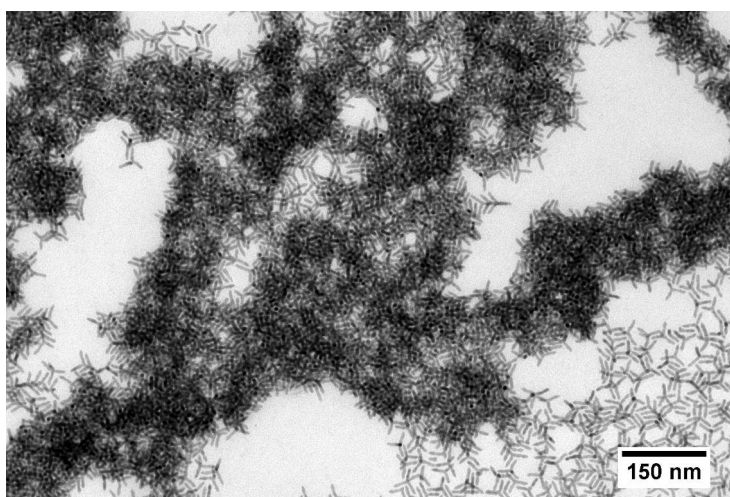


**Fig.S12.** *ZnTe@CdTe tetrapods drop-casted onto a TEM grid from ca. 0.3M PEG-MA (average  $M_n = 526$ , density of PEG-MA is 1.101 g/ml) solution in toluene.*



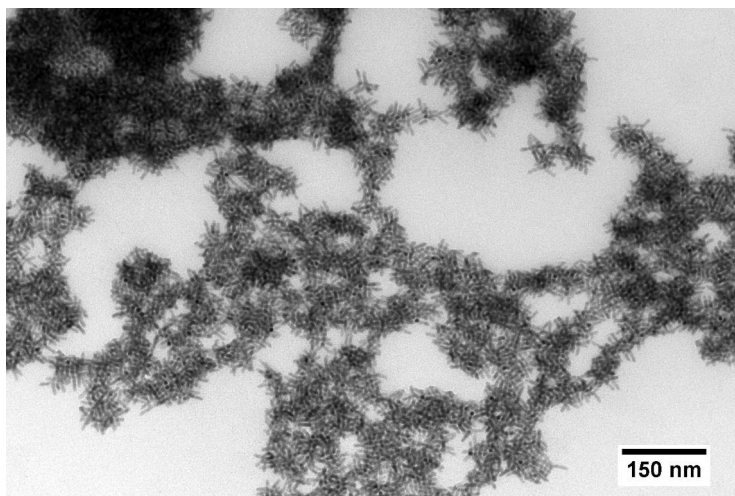


**Fig.S13.** *ZnTe@CdTe* tetrapods drop-casted onto a TEM grid from ca. **0.45 M** PEG-MA (average  $M_n = 526$ , density of PEG-MA is 1.101 g/ml) solution in toluene.

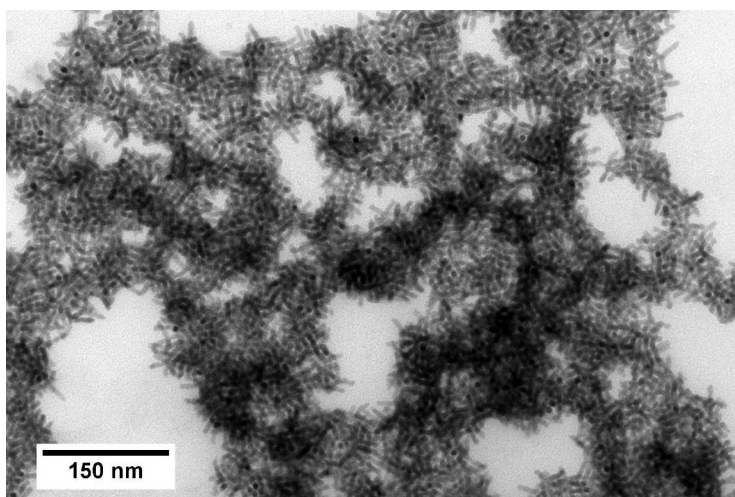


**Fig. S14.** *ZnTe@CdTe* tetrapods drop-casted onto a TEM grid from ca. **0.57 M** PEG-MA (average  $M_n = 526$ , density of PEG-MA is 1.101 g/ml) solution in toluene.

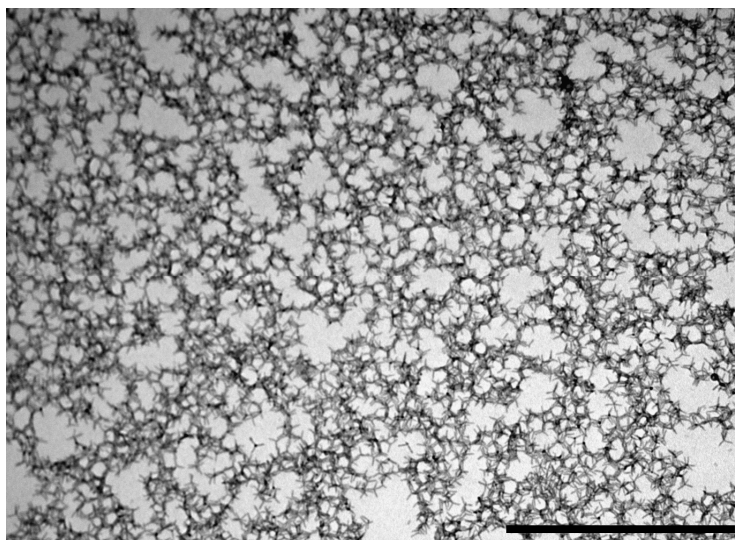


**Fig.S15.** TEM images of ZnTe@CdTe tetrapods networks obtained from toluene solution with PMMA (average  $M_w = 15\ 000$  g/mol). Scale bar is 1 micron.

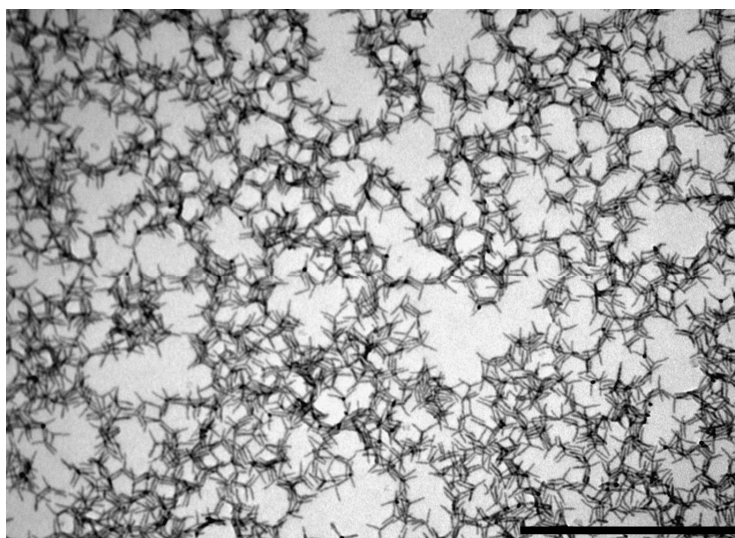


**Fig.S16.** TEM images of ZnTe@CdTe tetrapods networks obtained from toluene solution with PMMA (average  $M_w = 15\ 000$  g/mol). Scale bar is 500 nm.

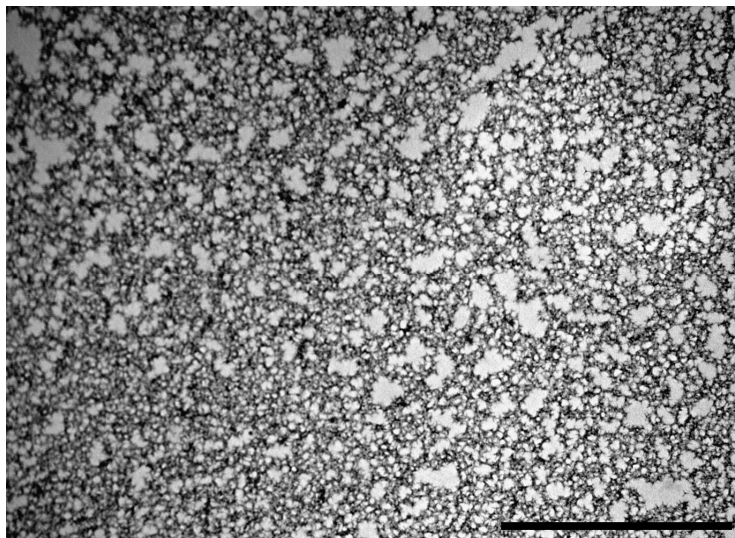


**Fig.S17.** TEM images of ZnTe@CdTe tetrapods networks obtained from toluene solution with PMMA (average  $M_w = 15\ 000$  g/mol). Scale bar is 2 micron.

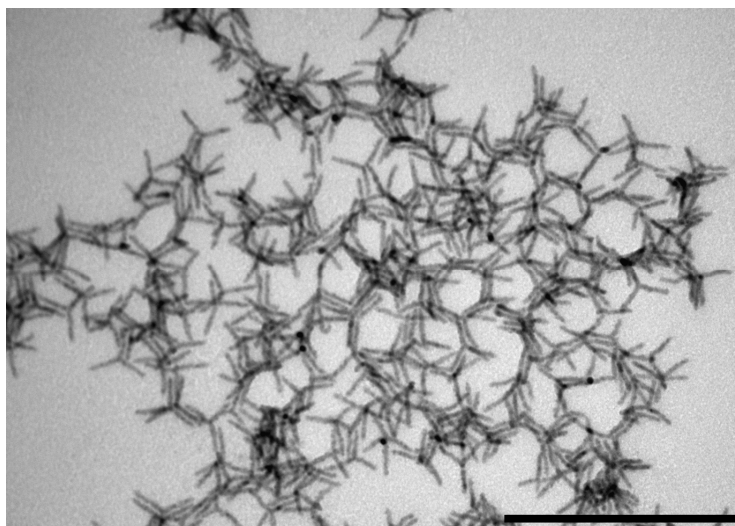


**Fig.S18.** TEM images of ZnTe@CdTe tetrapods networks obtained from toluene solution with PMMA (average  $M_w = 15\ 000$  g/mol). Scale bar is 200 nm.

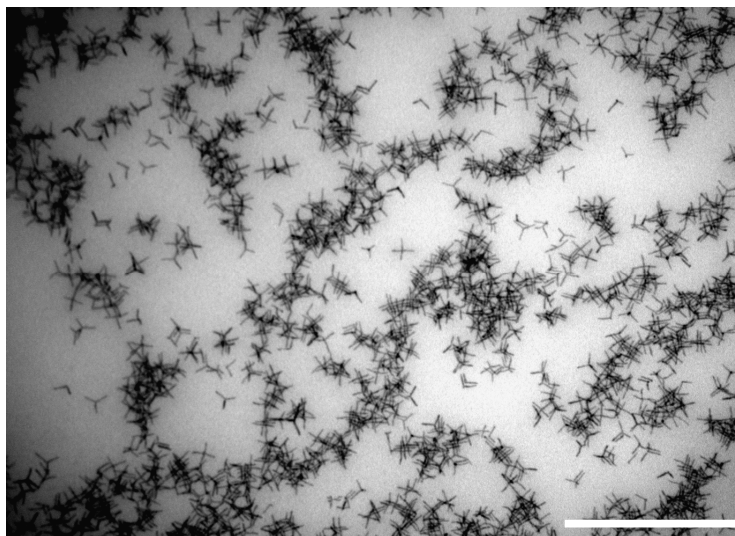


**Fig.S19.** TEM images of ZnTe@CdTe tetrapods interlacing each other as obtained from toluene solution with oleic acid. Scale bar is 500 nm.

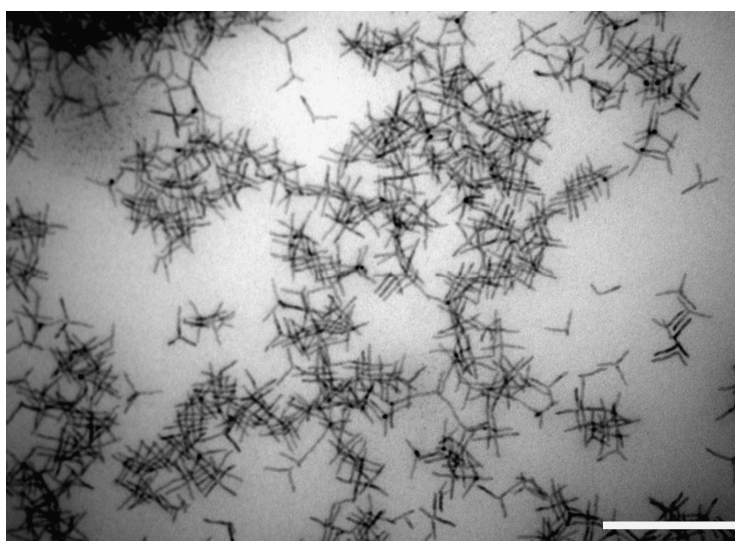


**Fig.S20.** TEM images of ZnTe@CdTe tetrapods interlacing each other as obtained from toluene solution with oleic acid. Scale bar is 200 nm.



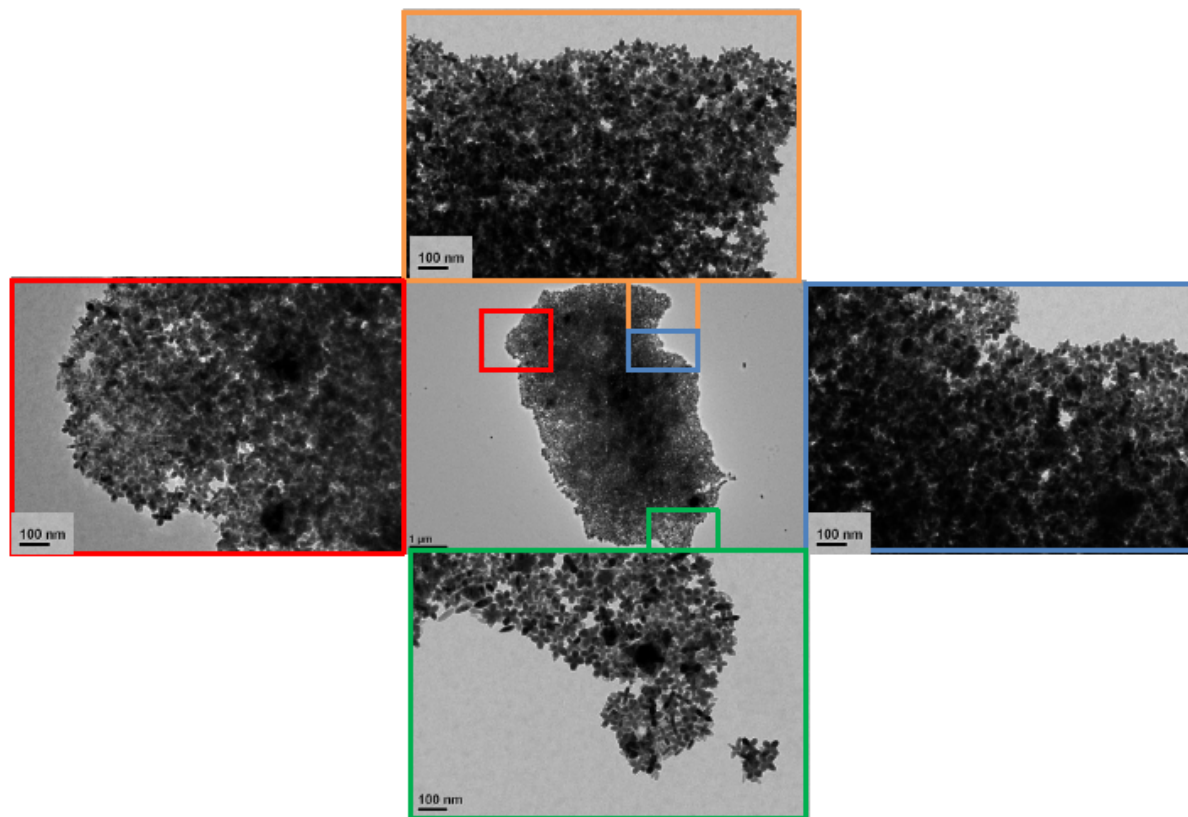


**Fig. S21.** TEM images of CdS octapods 3D assembly synthesized using oleic acid as additive. Higher magnification of some regions of the assembly are highlighted with different colors.

## References

- [1] Dmitry Baranov, Angela Fiore, Marijn van Huis, Cinzia Giannini, Andrea Falqui, Ugo Lafont, Henny Zandbergen, Marco Zanella, Roberto Cingolani and Liberato Manna, *Nano Lett.*, **2010**, *10* (2), pp 743–749.
- [2] Raffaella Buonsanti, Vincenzo Grillo, Elvio Carlino, Cinzia Giannini, Tobias Kipp, Roberto Cingolani and Pantaleo Davide Cozzoli, *J. Am. Chem. Soc.*, **2008**, *130* (33), pp 11223–112.
- [3] Jung-wook Seo, Young-wook Jun, Seung Jin Ko, and Jinwoo Cheon, *J. Phys. Chem. B*, **2005**, *109* (12), pp 5389–5391.
- [4] Masaki Saruyama, Masayuki Kanehara and Toshiharu Teranishi, *J. Am. Chem. Soc.*, **2010**, *132* (10), pp 3280–3282.
- [5] Bryce Sadtler, Denis O. Demchenko, Haimei Zheng, Steven M. Hughes, Maxwell G. Merkle, Ulrich Dahmen, Lin-Wang Wang, and A. Paul Alivisatos, *Journal of American Chemical Society*, **2009**, *131*, 5285–5293.